



CHALMERS
UNIVERSITY OF TECHNOLOGY

Integration of subcritical water extraction and treatment with xylanases and feruloyl esterases maximises release of feruloylated arabinoxylans from

Downloaded from: <https://research.chalmers.se>, 2024-12-20 16:14 UTC

Citation for the original published paper (version of record):

Jimenez Quero, A., Olsson, L. (2024). Integration of subcritical water extraction and treatment with xylanases and feruloyl esterases maximises release of feruloylated arabinoxylans from wheat bran. *Bioresource technology*. <http://dx.doi.org/10.1016/j.biortech.2024.130387>

N.B. When citing this work, cite the original published paper.



Integration of subcritical water extraction and treatment with xylanases and feruloyl esterases maximises release of feruloylated arabinoxylans from wheat bran

Reskandi C. Rudjito^a, Alvaro C. Matute^a, Amparo Jiménez-Quero^a, Lisbeth Olsson^{b,d}, Mary Ann Stringer^c, Kristian Bertel Rømer Mørkeberg Krogh^c, Jens Eklöf^c, Francisco Vilaplana^{a,e,*}

^a Division of Glycoscience, Department of Chemistry, KTH Royal Institute of Technology, AlbaNova University Centre, SE-106 91 Stockholm, Sweden

^b Division of Industrial Biotechnology, Department of Biology and Biological Engineering, Chalmers University of Technology, Kemivägen 10, 412 96 Gothenburg, Sweden

^c Novozymes A/S, Krogshøjvej 36, 2880 Bagsvaerd, Denmark

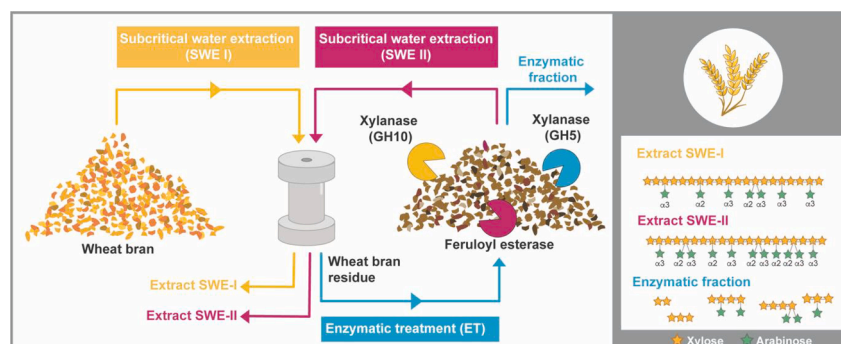
^d Wallenberg Wood Science Center, Chalmers University of Technology, Kemigården 4, 412 96 Gothenburg, Sweden

^e Wallenberg Wood Science Centre, KTH Royal Institute of Technology, Teknikringen 56-58, SE-100 44 Stockholm, Sweden

HIGHLIGHTS

- Integrated process with subcritical water and xylanolytic enzymes is developed.
- Up to 75% of extracted feruloylated arabinoxylan from wheat bran.
- Minimal enzyme cocktail with a xylanase and a feruloyl esterase is optimised.
- Arabinoxylans with tailored molar mass, substitution and feruloylation are obtained.

GRAPHICAL ABSTRACT



ARTICLE INFO

Keywords:

Hydrothermal treatment
Enzyme technology
Dietary fibre
Glycosyl hydrolases
Prebiotic oligosaccharides

ABSTRACT

Wheat bran is an abundant and low valued agricultural feedstock rich in valuable biomolecules as arabinoxylans (AX) and ferulic acid with important functional and biological properties. An integrated bioprocess combining subcritical water extraction (SWE) and enzymatic treatments has been developed for maximised recovery of feruloylated arabinoxylans and oligosaccharides from wheat bran. A minimal enzymatic cocktail was developed combining one xylanase from different glycosyl hydrolase families and a feruloyl esterase. The incorporation of xylanolytic enzymes in the integrated SWE bioprocess increased the AX yields up to 75%, higher than traditional alkaline extraction, and SWE or enzymatic treatment alone. The process isolated AX with tailored molecular structures in terms of substitution, molar mass, and ferulic acid, which can be used for structural biomedical applications, food ingredients and prebiotics. This study demonstrates the use of hydrothermal and enzyme

* Corresponding author at: Division of Glycoscience, Department of Chemistry, KTH Royal Institute of Technology, AlbaNova University Centre, SE-106 91 Stockholm, Sweden.

E-mail address: franvila@kth.se (F. Vilaplana).

<https://doi.org/10.1016/j.biortech.2024.130387>

Received 5 November 2023; Received in revised form 23 January 2024; Accepted 24 January 2024

Available online 29 January 2024

0960-8524/© 2024 The Authors. Published by Elsevier Ltd. This is an open access article under the CC BY license (<http://creativecommons.org/licenses/by/4.0/>).

technologies for upcycling agricultural side streams into functional bioproducts, contributing to a circular food system.

1. Introduction

Wheat bran (Wb), a by-product of milling, accounts for 14–16 % of wheat grain (Pomeranz, 1988) and contributes to around 120 million tons annually worldwide (FAO, 2021). This low cost feedstock is widely used as animal feed due to its insolubility and poor functional and organoleptic properties for human consumption (Prückler et al., 2014). However, the high polysaccharide and phenolic acid content of wheat bran deserves its potential upgrading into more profitable applications in the biomedical and nutritional sectors.

Arabinoxylan (AX) is a target component for wheat bran valorisation, an heterogenous polysaccharide enriched in the aleurone and pericarp layers, with 30–40 % dry weight (Reisinger et al., 2013). AX is composed of a (1 → 4)-linked-β-D-xylopyranosyl (Xylp) backbone with α-L-arabinofuranosyl (Araf) substitutions at the C(O)-3 and/or C(O)-2 positions (Izidorczyk and Biliaderis, 2000; Schooneveld-Bergmans et al., 1999). The arabinose can be further esterified to ferulic acid (FA) at the (O)-5 position (Gallardo et al., 2006), providing antioxidant properties and junction points for further enzymatic crosslinking (Mendez-Encinas et al., 2018). The unique structure of AX merits its application into multifunctional materials, such as films and hydrogels (Niño-Medina et al., 2009; Yilmaz-Turan et al., 2020), texturizing agents, and prebiotics (Grootaert et al., 2007).

Extraction of arabinoxylans from wheat bran is usually performed using aggressive alkaline conditions (Aguedo et al., 2014), reaching high yields between 45 and 70 % of AX (Li et al., 2020; Ruthes et al., 2017); however, alkaline conditions have the drawback of cleaving the ester bonds between the AX core and the valuable ferulic acid functionalities. In parallel, xylanolytic (xylan-degrading) enzymes can be used to selectively solubilise the AX present in wheat bran into oligosaccharides (Alokika and Singh, 2019; Santala et al., 2011), but these processes show usually low yields (between 5 and 10 % of the total AX) due to the recalcitrant cell wall structure (Aguedo et al., 2014; Santala et al., 2011), and drastically decrease the molar mass of the native AX required for functional properties. For structural and antioxidant food applications, it is important that the extracted AX exhibit a high molar mass and the ferulic acid is covalently attached to the polysaccharide core. This can be achieved using subcritical water extraction (SWE) (Li et al., 2020; Rudjito et al., 2019; Ruthes et al., 2017), which exploits the physicochemical changes of water at elevated temperature and pressure (below the critical point of 374 °C, 22 MPa). At these conditions, water exhibits lower polarity and viscosity, along with improved diffusivity (Peterson et al., 2008). The short extraction times, minimal downstream processing, possibility for recycling the solvent (water), non-requirement of catalysts, and preservation of functional groups make SWE an attractive and environmentally friendly mode of extraction. Nonetheless, SWE has its limitations; it is a relatively mild approach and in combination with the recalcitrance of wheat bran, only 20–25 % of the total AX content can be extracted (Aguedo et al., 2014; Li et al., 2020; Rudjito et al., 2019), and a substantial amount of AX remains unextracted in the wheat bran residue (Wb-R). In the wheat bran cell wall, AXs associate with other polysaccharides, proteins and lignin both covalently and non-covalently (Iiyama et al., 1994), whereby a portion of the covalent crosslinking is supported by di-ferulic acid (diFA), dimeric forms of ferulic acid that are commonly found in the form of 8-5', 8-O-4' and 5-5' diFA in wheat bran (Faulds et al., 2003). These diferulates contribute to cell wall inaccessibility and lower enzymatic degradability (Grabber et al., 1998), and presumably lower extractability of AX during SWE.

Enzymes can be used to selectively disintegrate the tight cell wall matrix in order to obtain unextractable AXs from recalcitrant Wb-R.

Xylanolytic enzymes typically used in xylan-rich feedstocks include endo-β-xylanases, β-xylosidases, α-glucuronidases, α-L-arabinofuranosidases and feruloyl esterases (Alokika and Singh, 2019). To achieve Wb-R relaxation, feruloyl esterases (FAE) from types A or D that can cleave both FA and diFA (Crepin et al., 2004), are essential as they break the junction points between intermolecular cross-linking. Inaccessibility due to tight packing in the cell wall can prevent FAEs from cleaving the phenolic bridges. Thus, synergistic help from other xylanolytic enzymes, such as endo-β-xylanases (X), is often needed (Faulds et al., 2004; Ruthes et al., 2017).

Xylanases from glycoside hydrolase (GH) family 10 exhibit the broadest specificity, being able to accommodate linear xylan and Araf substitutions at the -2 and +1 subsites (Pollet et al., 2010). Xylanases from GH11 are more restricted by substitution, generally allowing Araf substitutions at the +2 subsite (Paës et al., 2012), while the GH5s prefer highly substituted AX, requiring specific Araf motifs as a specificity determinant for cleavage (Correia et al., 2011). Hence, a minimal enzymatic cocktail consisting of a FAE in combination with an endo-β-xylanase from two distinct GH families (GH10 and GH5), was screened and optimised to further target the insoluble and recalcitrant Wb-R obtained after SWE (Fig. 1). By using an array of chromatographic approaches, the performance, and products from each process step i.e., first round of SWE (SWE I), enzymatic treatment (ET) and second round of SWE (SWE II), were analysed in depth to determine the optimal process conditions, as well as to better understand enzyme activity in insoluble recalcitrant wheat bran substrates, and the effect of process steps on the molecular structure of the solubilised AXs and oligosaccharides. This integrated bioprocess contributes to a maximised valorisation of AX from wheat bran towards its utilisation in biomedical and nutritional applications.

2. Materials and methods

2.1. Materials

Wheat bran (Wb) was provided by Lantmännen (Stockholm, Sweden) and was further destarched (dWb) prior to subcritical water extraction (SWE). The composition and structure of dWb are shown in Table 1. All the chemicals were of analytical grade (Sigma Aldrich, Stockholm, Sweden), unless otherwise stated.

2.2. Enzymes

Endo-β-1,4-xylanases of GH11 from *Thermomyces lanuginosus* (TlXyn11), GH10A from *Aspergillus aculeatus* (AcXyn10A), GH10B appended to CBM1 from *Aspergillus aculeatus* (AcXyn10A CBM1), GH10B from *Aspergillus aculeatus* (AcXyn10B), GH5_21 appended to CBM13 from *Chryseobacterium* sp-10696 (CXyn5_21 CBM13), GH5_34 from *Gonapodya prolifera* (GpXyn5_34) and type D feruloyl esterase appended to CBM1 from *Magnaporthe grisea* (MgFAE1D CBM1) were provided by Novozymes A/S (Bagsværd, Denmark). All enzymes were expressed in host strains optimized for heterologous production.

2.3. Bioprocess optimisation and validation

2.3.1. Pilot-scale subcritical water extraction of destarched wheat bran

Wheat bran residue (Wb-R) was obtained from a pilot-scale sequential subcritical water extraction (SWE) using a 5L rotary autoclave submerged in a polyethylene glycol (PEG) bath (Yilmaz-Turan et al., 2020). The composition and structure of Wb-R are shown in Table 1. The SWE was performed using destarched wheat bran (dWb) at

160 °C for 5 min then 30 min, respectively. The Wb-R was then recovered, washed with water, freeze-dried, and kept at -20 °C until further use.

2.3.2. Enzymatic end-point screening on wheat bran residue using single xylanases

The screening aimed to compare the maximum solubilisation from Wb-R using end point incubations. Wb-R was suspended in phosphate

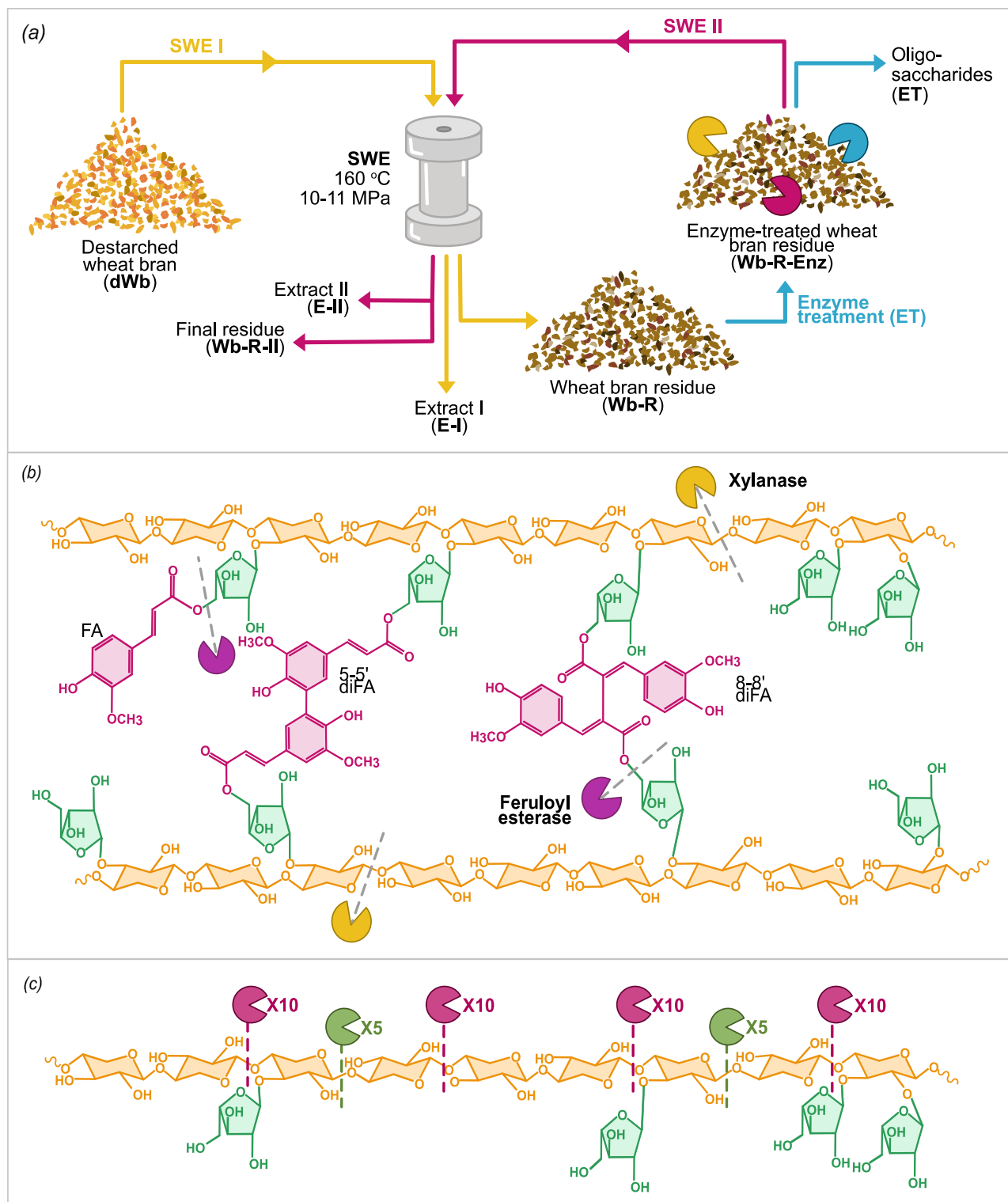


Fig. 1. Illustrative overview of the integrated bioprocess for maximised release of feruloylated arabinoxylans (AX) from wheat bran. (a) Bioprocess scheme comprised of a first cycle of subcritical water extraction I (SWE I) in yellow, followed by enzymatic treatment (ET) in blue and a second cycle of SWE (SWE II) in pink. (b) Structure of a crosslinked AX with marked cleavage sites for xylanases and feruloyl esterases. (c) Proposed cleavage sites of xylanases from glycoside hydrolase (GH) family 10 and 5. Note SWE: subcritical water extraction, FA: ferulic acid, diFA: diferulic acid and X: xylanase. (For interpretation of the references to colour in this figure legend, the reader is referred to the web version of this article.)

Table 1
Composition of wheat bran substrates.

	Destarched wheat bran (dWb)	Wheat-bran residue (Wb-R)
Carbohydrate content (mg g⁻¹DW)^a	686.3 (12.8)	554.3 (3.3)
Rha (%)	-	-
Fuc (%)	-	-
Ara (%)	200.0 (6.5)	118.3 (0.9)
Xyl (%)	260.7 (1.7)	187.9 (1.0)
Gal (%)	14.2 (0.1)	10.8 (0.1)
Glc (%)	210.0 (4.4)	237.4 (1.2)
Man (%)	-	-
AX (%)	67.1 (1.0)	55.2 (0.6)
AX (mg g ⁻¹ DW)	460.6 (8.3)	306.2 (1.9)
A/X ^b	0.76	0.63
t-Xylp ^c	2	10
4-Xylp ^c	80	68
2,4-Xylp ^c	2	4
3,4-Xylp ^c	10	9
2,3,4-Xylp ^c	6	10
Phenolic acid (mg g⁻¹DW)^d	5.7 (0.1)	2.8 (0.6)
p-Coumaric (mg g ⁻¹ DW)	0.1 (0.01)	0.07 (0.03)
Ferulic (mg g ⁻¹ DW)	5.5 (0.1)	2.4 (0.4)
8-8' diFA (mg g ⁻¹ DW)	0.07 (0.01)	0.23 (0.1)
5-5' diFA (mg g ⁻¹ DW)	0.1 (0.01)	0.2 (0.1)

^aCarbohydrate content was determined using sulfuric acid hydrolysis followed by HPAEC-PAD analysis.

^bA/X is the ratio between Ara and Xyl.

^cSubstitution pattern of xylan backbone from glycosidic linkage analysis. Nomenclature as in Fig. 5a.

^dPhenolic acid content was determined by saponification followed by HPLC analysis.

buffer (pH 6.5, 20 mM) at 5 mg/ml and 1 mg enzyme/g substrate of each *endo*- β -1,4-xylanase (*TLXyn11*, *AcXyn10A*, *AcXyn10A* CBM1, *AcXyn10B*, *CXyn5_21* CBM13, *GpXyn5_34*) was added to the Wb-R suspension. The enzyme dosage was selected based on previous kinetic information on soluble AX fractions (Rudjito et al., 2023). The enzymatic reactions were incubated at 37 °C for 48 h with agitation at 30 rpm using the IKA Loopster digital (IKA, Staufen, Germany). After 6 h, 24 h, and 48 h, aliquots of the reactions were transferred to new microcentrifuge tubes (Eppendorf, Germany). The reactions were inactivated at 95 °C for 10 min and kept at 4 °C until further use. The *TLXyn11* was thermostable and was instead pH inactivated. A negative control was prepared by replacing the enzyme with buffer. All the reactions were performed in triplicate.

2.3.3. Enzymatic screening using a combination of xylanase and feruloyl esterase

From the screening of single xylanases, one enzyme from each family (*TLXyn11*, *AcXyn10A* CBM1, *CXyn5_21* CBM13) was selected and combined with a feruloyl esterase (*MgFAE1D* CBM1) for a second round of screening on Wb-R. Using the same conditions as the single xylanase screening, 5 mg/ml of Wb-R was prepared in phosphate buffer (pH 6.5, 20 mM) and 1 mg enzyme/g substrate of selected xylanase and feruloyl esterase was added to the suspension. The reactions were incubated at 37 °C for 48 h and aliquots were obtained at 6 h, 24 h and 48 h, where they were further inactivated. We aimed a negative control was prepared by replacing the enzyme with an equal volume of buffer. All the reactions were performed in triplicate.

2.3.4. Enzymatic treatment of wheat bran residue

Based on the results of the enzymatic screenings, selected enzyme combinations (*AcXyn10A* CBM13 with *MgFAE1D* CBM1 and *CXyn5_21* CBM13 with *MgFAE1D* CBM1) were implemented on a larger amount of Wb-R (7 g). Here, MilliQ water was used instead of buffer to omit the need for dialysis and a lower enzyme load of 0.1 mg enzyme/g substrate was used. Otherwise, the reactions occurred in the same temperature of

37 °C for 48 h, with agitation at 150 rpm using a shaker incubator (Infors HT, Bottmingen, Switzerland). After enzymatic treatment, the suspensions were centrifuged at 3000 rpm for 10 min and the supernatant was transferred and freeze-dried for further analysis (DNSA, oligosaccharide analysis using HPAEC-PAD and ESI-MS). The pellet was washed 3 times with ethanol 95 % (v/v), using centrifugation in between, and oven-dried overnight prior to subcritical water extraction (SWE II). The dry weight of the supernatant and pellet fractions were then used to determine the yields of the enzymatic treatment. The water content of the Wb-R was determined by the gravimetric difference before and after freeze-drying in triplicate.

2.3.5. SWE of destarched wheat bran (SWE I) and enzyme-treated residual wheat bran (SWE II)

For SWE I, a sequential extraction was performed on dWb at laboratory scale to simulate the pilot-scale extraction performed previously (Yilmaz-Turan et al., 2020), as well as the initial step of the integrated bioprocess. Briefly, 3 g of dWb was subjected to subcritical water extraction using an Accelerated Solvent Extraction Dionex™ ASE™ 350 (Thermo Fisher Scientific Inc., USA), as previously described (Ruthes et al., 2017). The sample was placed into the extraction cell that has been lined with Dionex ASE Prep DE Diatomaceous Earth (Thermo Fisher Scientific, Stockholm, Sweden) sandwiched in between ASE Extraction Cellulose Filters (Thermo Fisher Scientific, Stockholm, Sweden). The prepped cells were then subjected to a sequential extraction at 160 °C for 5 and 30 min using MilliQ water as the solvent. For SWE II, 3 g of the enzyme treated residual wheat bran was subjected to a single cycle of SWE at 160 °C for 15 min, using MilliQ water as the solvent. During extraction, the ASE maintained a pressure of 10–11 MPa and a solid to liquid ratio of 1:14 (w/v). Both the extract and remaining residue were then collected and freeze-dried for further analysis. The yields of extraction were calculated from the dry weights of the extracts and remaining residue. The extractions were performed in duplicate.

2.4. Analysis of enzymatic hydrolysates and SWE fractions

2.4.1. Monosaccharide analysis by acid hydrolysis and HPAEC-PAD

Insoluble fractions were hydrolysed using the two-step sulfuric acid hydrolysis (Saeman et al., 1954), followed by HPAEC-PAD analysis (McKee et al., 2016). For the enzyme treated Wb-R, suspensions were centrifuged at 3000 rpm for 10 min to separate the soluble (oligosaccharides) and insoluble (treated Wb-R) fractions. The insoluble pellet was washed 3 times with water, with centrifugation in between, transferred into glass tubes, freeze-dried, weighed and subjected to sulfuric acid hydrolysis. Analysis was performed in triplicate.

The soluble extracts were hydrolysed by trifluoroacetic acid (TFA) hydrolysis, followed by analysis of the released monosaccharides by HPAEC-PAD. In summary, 1 mg samples were hydrolysed with 1 ml of 2 M TFA at 120 °C for 3 h. The hydrolysates were dried under a stream of air, re-suspended in water and analysed on a ICS6000 fitted with a Dionex CarboPac PA1 IC column (Thermo Scientific, Stockholm, Sweden), as previously described (McKee et al., 2016). Analysis was performed in triplicate.

2.4.2. Reducing sugar assay

Reducing sugar released after enzymatic treatment was measured on the soluble fraction using the 3,5-dinitrosalicylic acid (DNSA) assay (Miller, 1959) with modifications (McKee, 2017). The DNSA assay was adjusted to a 96-well microplate and analysed using the Clariostar microplate reader (BMG Labtech, Germany) in triplicate. To quantify the reducing sugar content, a calibration curve was constructed using xylose at 0.1–1.0 mg/ml.

2.4.3. Analysis of oligosaccharides using HPAEC-PAD

Samples were analysed using the Dionex CarboPac PA200 column fitted into the ICS6000 system (Dionex Sunnyvale, CA, USA). Separation

was achieved using the method previously described by Falck et al. (2014). A standard mixture composed of monosaccharides (arabinose and xylose) and oligosaccharides (X_2 , X_3 , X_4 , X_5 , X_6 , A^3X , A^2XX , $A^{2,3}XX$ and XA^2XX/XA^3XX) from Megazyme (Wicklow, Ireland) was used as reference.

2.4.4. Oligosaccharide mass profiling (OLIMP)

OLIMP was performed using electrospray ionization (ESI) coupled to a Synapt G2 mass spectrometer (Waters Corporation, Milford, MA, USA). Samples were diluted in acetonitrile 50 % (v/v) with 0.1 % (v/v) formic acid to 0.1 mg/ml and filtered through Chromacol 0.2 μ m filters (Scantec Nordic, Sweden) and directly injected into the ESI-MS. The capillary and cone voltage were set to 3 kV and 70 kV, respectively. The oligosaccharides were detected as $[M + Na]^+$ adducts.

2.4.5. Size exclusion chromatography

The molar mass distribution of the extracts was determined using the SECurity 1260 size exclusion chromatography (Polymer Standard Services, Mainz, Germany) coupled to a refractive index, as formerly described (Ruthes et al., 2017). Samples were solubilised in water containing 100 mM $NaNO_3$ and 5 mM NaN_3 .

2.4.6. Glycosidic linkage analysis

Glycosidic linkage analysis was performed in triplicate by per-*O*-methylation of the samples, followed by acid hydrolysis, derivatisation and analysis by GC-MS (Pettolino et al., 2012). The mol percentages (% mol) of identified partially methylated alditol acetates (PMAA) obtained from the analysis were corrected to the monosaccharide content of each sample. Analysis was performed in triplicate.

2.4.7. Phenolic acid content

Phenolic acids were released by saponification followed by analysis using HPLC (Antoine et al., 2003; Comino et al., 2014). Samples (10 mg) were saponified with 500 μ l of 2 M NaOH at either 30 $^{\circ}C$ (for soluble extracts) or 80 $^{\circ}C$ (for insoluble bran) for 17 h, with agitation in duplicate. The saponified samples were then acidified to pH 3.0 using 12 M HCl, partitioned with ethyl acetate and dried under nitrogen. The dried phenolic acid fractions were resuspended in methanol:2 % (v/v) acetic acid (1:1, v/v), filtered through Chromacol 0.2 μ m filters (Scantec Nordic, Sweden) and analysed on the HPLC using the ZORBAX StableBond C18 column (Agilent Technologies, USA) fitted with photodiode array detection at 200–400 nm (Waters 2695, MA, USA). Samples that were not saponified were diluted with methanol:2 % (v/v) acetic acid (1:1, v/v), filtered through Chromacol 0.2 μ m filters (Scantec Nordic, Sweden) and subjected to the HPLC for analysis. The phenolic acids were separated in accordance to a previous method (Menzel et al.,

2019). To confirm the presence of diferulic acids that do not correspond to available standards, samples were analysed using LC-ESI-MS as previously described (Rudjito et al., 2020; Vismeh et al., 2013).

3. Results and discussion

3.1. Initial SWE releases high molar mass feruloylated AX from Wb with low substitution

The main aim of this study was to combine selective enzymatic treatments together with SWE to maximise the solubilisation of recalcitrant AX from wheat bran. The first step of the process was to perform SWE I, which is an effective approach to extract accessible feruloylated AX with high purities and preserving high degree of feruloylation and molar mass (Rudjito et al., 2019). Here, we performed SWE I sequentially for 5 and 30 min at 160 $^{\circ}C$ on destarched wheat bran (dWb). Typical trends were observed from the extracts, marked by the enrichment of AX and increased complexity of the AX structure (A/X ratio and phenolic acid content) in respect to increased extraction time (Fig. 2, see supplementary materials). The 30-min extract of SWE I (E-I-30') was enriched with 635 mg/g of AX, exhibited an A/X ratio of 0.3, FA content of 12 mg/g and was obtained with a reasonable yield of 14 % dry weight. The fractions obtained from SWE I can ideally be purified to remove small molecular weight compounds and non-AX polysaccharides, for example glucans that constituted 141 mg/g of the extract.

SWE I generally yielded a substantial amount of AX with high purities after several cycles of extractions. However, 43 % of AX remained in the residual biomass after SWE I, revealing the presence of recalcitrant AX that could not be released using SWE I alone. Prolonged exposure at subcritical conditions also leads to autohydrolysis, resulting in degradation of the polymeric AXs and the release of Araf substitutions (Ruthes et al., 2017).

There is a fine balance between the amount of extractable AXs from SWE and the effect of SWE on the structure of the extracted AXs. In respect to increased extraction time, the extracted AXs were more substituted with higher A/X ratio and FA content, suggesting that complexity increases with recalcitrance (Rudjito et al., 2019). Therefore, the remaining AXs in Wb-R was hypothesised to be heavily substituted and crosslinked. By using enzymes prior to SWE II, selective cleavage of diFA bridges (AX to AX and/or lignin and protein) was targeted using a feruloyl esterase and xylanase, in order to disrupt the tight and recalcitrant structure in Wb-R and to reduce the need for longer extraction times in SWE II.

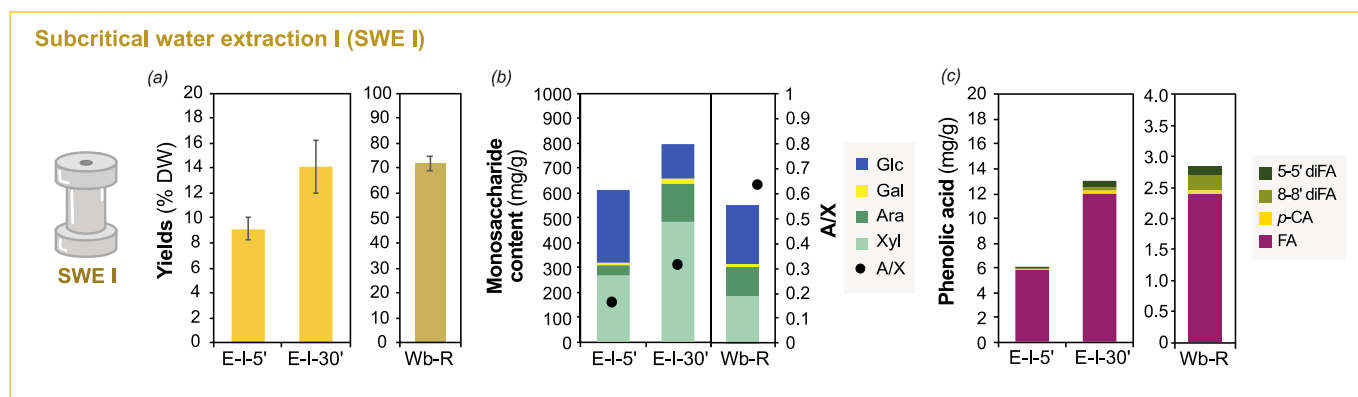


Fig. 2. Subcritical water extraction I (SWE I). (a) Yields of extracts and residues in percentage dry weights (% DW). (b) Monosaccharide content of extracts and residue together with their respective arabinose to xylose (A/X) ratios. (c) Phenolic acid content of extracts and residue released after saponification. Note E-I: extract from SWE I and Wb-R: wheat bran residue, Glc: glucose, Gal: galactose, Ara: arabinose, Xyl: xylose, FA: ferulic acid, pCA: *p*-coumaric acid and diFA: di-ferulic acid.

3.2. Xylanases partially solubilise Wb-R while enriching the insoluble fraction with highly substituted AX

The first screening procedure on Wb-R was performed using single xylanases from GH families 11, 10 and 5. Here, the Wb-R used for the enzymatic treatments originated from a pilot-scale SWE that was performed in a previous study (Yilmaz-Turan et al., 2020). The monosaccharide composition of the Wb-R from the pilot-scale SWE and that of SWE I performed in this study were very similar (see Table 1 and supplementary materials). As shown from the release of reducing sugars in Fig. 3a, at 6 h the xylanases from GH10 and 11 resulted in similar values, but at 48 h the AcXyn10A CBM1 resulted in the highest release at 233 mg/g AX. Contrarily, the GH5 xylanases resulted in the lowest release of reducing sugars. It should be noted that the reducing sugar assay does not consider the size and type of hydrolysis products and the results shown only give an overview of their relative activity. Hydrolysis

products released by GH10 and 11 xylanases are generally smaller than those by GH5s (Pollet et al., 2010), which explain the higher release of reducing sugars.

The insoluble fractions were then analysed in terms of their monosaccharide content (Fig. 3b), and the results revealed that the A/X ratio significantly increased after xylanase treatment in all cases, especially in the Wb-R treated with AcXyn10A CBM1. In this sample the A/X ratio rose from 0.6 (Wb-R) to 1.2, meaning that the remaining AX in the enzyme treated Wb-R was heavily substituted. The GH10 xylanases can generally tolerate highly substituted AXs, as it can accommodate Araf substitutions at the -2 and +1 subsites (Pollet et al., 2010). However, at an A/X ratio of 1.2, likely all the xyloses on the AX backbone carry at least one Araf substitution, which hinder further cleavage by the AcXyn10A CBM1. Interestingly, the residues treated after GH5_21 and GH5_34 had lower A/X ratio than those treated by GH10 and GH11 counterparts, which confirmed their preference towards substituted

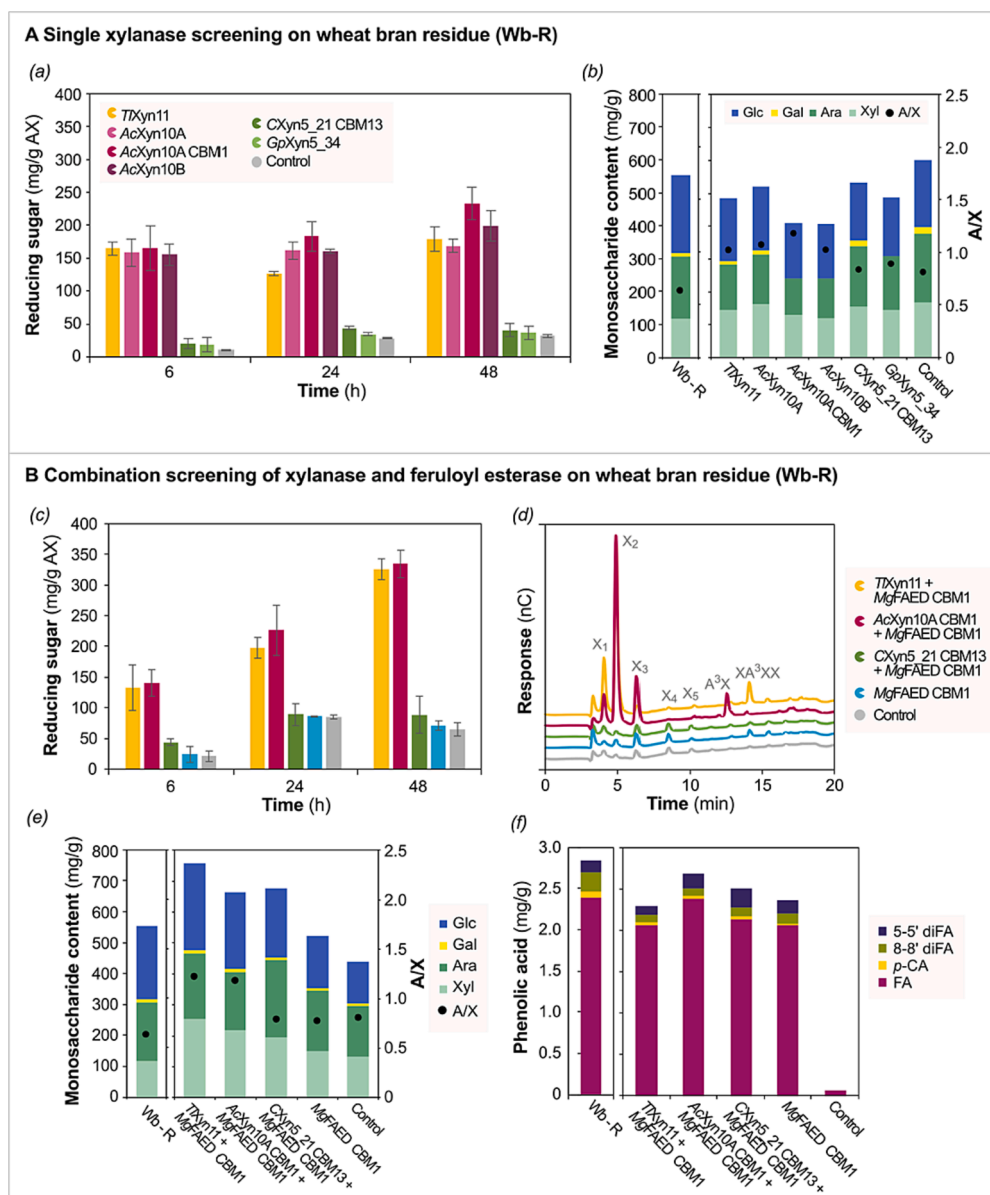


Fig. 3. Enzymatic screening on wheat bran residue (Wb-R). (a) Release of reducing sugars by single xylanases. (b) Monosaccharide content of Wb-R before and after treatment with single xylanases. (c) Release of reducing sugars by xylanase and feruloyl esterase. (d) HPAEC-PAD profiles of released oligosaccharides by xylanase and feruloyl esterase after 48 h. (e) Monosaccharide content of Wb-R before and after treatment with xylanase and feruloyl esterase. (f) Phenolic acid content of Wb-R and hydrolysates enzymatically released after 48 h. Note Glc: glucose, Gal: galactose, Ara: arabinose, Xyl: xylose, A/X: arabinose to xylose ratio, FA: ferulic acid, pCA: p-coumaric acid and diFA: di-ferulic acid.

portions in the AX backbone.

3.3. Xylanases work synergistically with feruloyl esterase to partially degrade Wb-R

Based on the results of the single screenings, one xylanase from GH family 11, 10 and 5 was then chosen for the combined screening with MgFAE1D CBM1. This feruloyl esterase was pre-selected for its ability to cleave both FA and diFA from feruloylated arabinoxylan substrates, belonging to type D FAE (Crepin et al., 2004). From the release of reducing sugars (Fig. 3c), the combination of xylanase and feruloyl esterase resulted in an increased value compared to treatment with only xylanase (Fig. 3a), signifying their synergy. This emphasizes that with the removal of phenolic acids, the xylanases can delve their way deeper into the Wb-R and further hydrolyse released arabinoxylan oligosaccharides that no longer carry phenolic acids moieties. Similar to the single screening, the AcXyn10A CBM1 (in combination with MgFAE1D CBM1) resulted in the highest release of reducing sugars at 335 mg/g AX, after 48 h of incubation. In fact, both AcXyn10A CBM1 and TlXyn11 in combination with MgFAE1D CBM1 displayed high release of reducing sugars, much more than the CXyn5_21 CBM13. The higher reducing sugar content by AcXyn10A CBM1 and TlXyn11 was attributed to the high abundance of small xylooligosaccharides, specifically X₁-X₃ (Fig. 3d). The CXyn5_21 CBM13, though it released low amounts of detectable oligosaccharides, was still an interesting candidate for the bioprocess as it prefers highly substituted substrates, requiring a C(O)-3 linked Araf substitution for cleavage (Rudjito et al., 2023). Minimal cleavage on the AX backbone by CXyn5_21 CBM13 can additionally benefit production of longer hydrolysis products.

The enzyme treated Wb-R samples were further analysed in terms of their monosaccharide content, and once again the A/X ratios increased after enzymatic treatment (Fig. 3e). The most noticeable increase in the A/X ratio was observed in TlXyn11 and AcXyn10A CBM1 (both in combination with MgFAE1D CBM1), which exhibited A/X values of 1.2, respectively, and less for the GH5 enzymes. It seemed that addition of MgFAE1D CBM1 on Wb-R, increased accessibility for TlXyn11 compared to AcXyn10A CBM1, as in the latter, the A/X ratio did not change after the addition of MgFAE1D CBM1. It has been well reported that the GH10 xylanases are more tolerant towards substitution than the GH11 (Pollet et al., 2010), and this highlights the impact of phenolic acid removal on the activity of the GH11.

Moreover, the total released phenolic acids were quantified in comparison to the total phenolic acid present in Wb-R, which was measured after saponification (Fig. 3f). It should be noted that the measured phenolic acid content in Wb-R is presumably underestimated, as not all the present diFAs could be quantified due to the lack of standards. Considering this notion, the MgFAE1D CBM1 alone and in combination with the different xylanases released most of the phenolic acids measured in Wb-R. The AcXyn10A CBM1 in combination with MgFAE1D CBM1 released the highest amount of total phenolic acids, especially monomeric FA. In addition, more 5-5' diFA was released by MgFAE1D CBM1 in combination with AcXyn10A CBM1 than TlXyn11, which was similarly reported by Faulds et al. (2006). The lower release of the 8-8' diFA by MgFAE1D CBM1 could be explained by its tighter chemical conformation than the 5-5' diFA, resulting in a more compressed molecular arrangement with the AXs, thus less accessibility for cleavage.

For subsequent enzymatic treatment at larger scale, we selected the combination of AcXyn10A CBM1 with MgFAE1D CBM1 and CXyn5_21 CBM13 with MgFAE1D CBM1, based on their activity and the presence of carbohydrate binding modules (CBM). The CBM1 of fungal enzymes are known to bind to crystalline cellulose (Lehtio et al., 2003), while the CBM 13 appended to a xylanase 10A from *Streptomyces lividans* exhibited binding to xylan as well as small sugars (Notenboom et al., 2002). The presence of CBMs was predicted to enhance the effective enzyme concentration on the insoluble surface of the Wb-R. In terms of activity, the

AcXyn10A CBM1 was undoubtedly superior and with the addition of MgFAE1D CBM1, the cocktail could release the highest amounts of phenolic acids. Meanwhile for CXyn5_21 CBM13, even though not much reducing sugars or oligosaccharides were released in the soluble hydrolysate, we hypothesized that its preference towards highly substituted AXs would benefit Wb-R relaxation.

3.4. Enzymatic treatment aided release of oligosaccharides and relaxation of Wb-R

From the screening, the combinations AcXyn10A CBM1 with MgFAE1D CBM1 and CXyn5_21 CBM13 with MgFAE1D CBM1 were chosen for the larger scale enzymatic treatment, which was then followed by SWE II. For simplicity, these combinations will be termed X10A-F and X5_21-F, respectively, from this point on. The enzymatic treatment on this scale was performed with a lower enzyme load (10 times less) due to enzyme availability; nevertheless, the amount of released reducing sugar was still comparable to that of the screenings in the end point (Fig. 4a). In terms of yields, the soluble fraction from the enzymatic treatment using X10A-F (ET-X10A-F), which was composed of the initial supernatant and washes of the treated Wb-R, was higher than the ET-X5_21-F (Fig. 4b, see supplementary materials). The ET-X10A-F was mainly composed of unsubstituted xylo-oligosaccharides with a low A/X ratio of 0.2 (Fig. 4c). Indeed, the HPAEC-PAD profile revealed that ET-X10A-F contained large amounts of xylobiose (X₂) constituting 30 % of the total xylose content (Fig. 4d). In contrast, ET-X5_21-F showed less release of xylooligosaccharides with a higher A/X ratio of 0.3. It was anticipated that CXyn5_21 CBM13 would release more substituted oligosaccharides due to its specificity, thus explaining the higher A/X. The treated Wb-Rs exhibited a similar outcome to that of the screenings, where Wb-R-X10A-F was markedly enriched with highly substituted AXs, more so than Wb-R-X5_21-F (Fig. 4c).

The overall amount of released phenolic acids during enzymatic treatment were comparable to those of the screening (Fig. 4f), with higher release of phenolic acids by X10A-F compared to X5_21-F. The release of 5-5' diFA was again more prominent than 8-8' diFA in both enzymatic treatments. Additionally, by measuring both free and bound phenolic acids in the hydrolysates, we could highlight that a substantial portion of the phenolic acids were still esterified to the released oligo- and polysaccharides, inferring that they were not completely cleaved off by the MgFAE1D CBM1. Based on the oligosaccharide mass profiling (Fig. 4e), longer feruloylated AX oligosaccharides were observed in ET-X5_21-F (up to P7F), as compared to ET-X10A-F (up to P4F). Meanwhile, in the treated Wb-Rs, the residues were enriched in diFAs, particularly the 5-5' diFA, which suggests their increase in recalcitrance.

Following enzymatic treatment, Wb-R-Enz was subjected to a second round of SWE (SWE II), while Wb-R (directly from SWE I) was tested as control (E-II-C). The extract yields from SWE II (E-II) were highest for E-II-X10A-F, followed by E-II-C and E-II-X5_21-F (Fig. 4g). In terms of monosaccharide composition, E-II-X10A-F and E-II-X5_21-F were mainly composed of AX, while E-II-C contained slightly more mixed linked β -glucans (Fig. 4h). Mixed linked β -glucans are generally more extractable than AX (Rudjito et al., 2019), so they were likely co-extracted during the enzyme treatment for Wb-R-X10A-F and Wb-R-X5_21-F.

As for the phenolic acid content of the SWE II extracts, a prominent release of monomeric FA was observed in E-II-C, while in E-II-X10A-F and E-II-X5_21-F, the extracts contained more 8-8' diFA and 5-5' diFA than in E-II-C (Fig. 4i). In comparison to the phenolic acid content of E-I-30', the E-II-X10A-F contained twofold the amount of both diFAs (5-5' and 8-8' diFA), inferring that the diFAs were more susceptible in SWE II after enzymatic treatment. The release of diFA suggests that the enzymes were able to partly cleave diFA bridges and/or cleave the AX backbone in close proximity to the diFAs. Both events would result in opening up the recalcitrant network organisation of Wb-R and thus release of extractable feruloylated AX during SWE II. For both E-II-C and E-II-

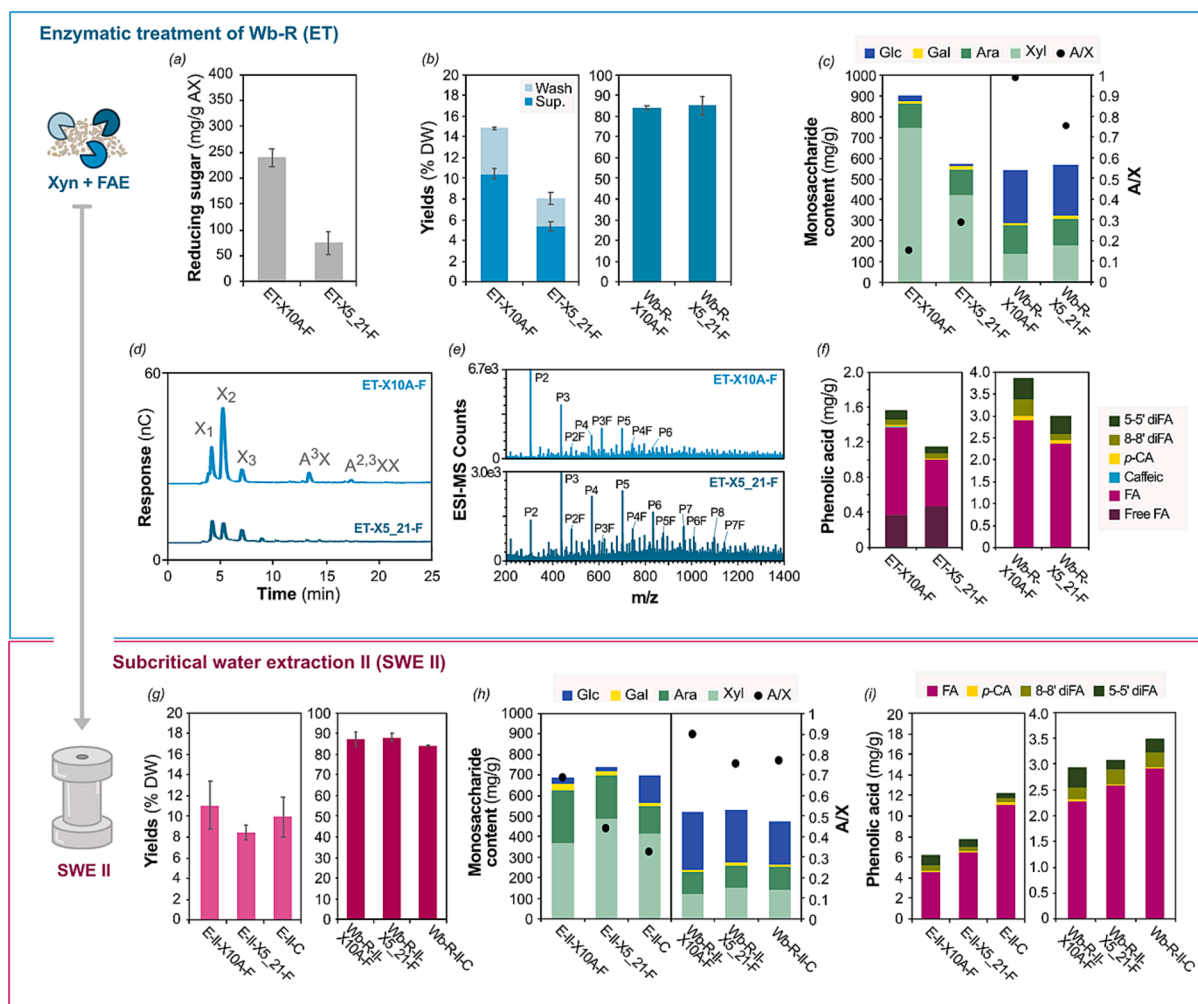


Fig. 4. Combining enzymatic treatment (ET) prior to subsequent subcritical water extraction (SWE II). Outcome of ET at larger scale, shown in terms of the (a) released reducing sugars, (b) yields of hydrolysate (supernatant and wash) and treated Wb-R, (c) monosaccharide content, (d) HPAEC-PAD profiles of released oligosaccharides, (e) oligosaccharide mass profiling (OLIMP) of released oligosaccharides and (f) phenolic acid content. Outcome from SWE II of enzyme-treated Wb-R in terms of (g) yields, (h) monosaccharide content and (i) molar mass distribution. Note E-II: extract from SWE II, R-II: residue from SWE II, C: control, X: xylanase, F: feruloyl esterase, Glc: glucose, Gal: galactose, Ara: arabinose, Xyl: xylose, FA: ferulic acid, pCA: *p*-coumaric acid and diFA: di-ferulic acid.

X5_21-F, more monomeric FA was found in the extracts than in E-II-X10A-F. This is explained by the fact that less phenolic acids were recovered in ET-X5_21-F, while none was recovered for the Wb-R control. Hence, compounds that were not extracted in the previous step, were evidently more easily released in the next steps of the bioprocess.

3.5. The integrated bioprocess enables solubilization of AX with varying molecular structures

To provide a deeper understanding of the fractions obtained from the different steps of the bioprocess, glycosidic linkage and molar mass analysis were performed on the soluble enzymatic hydrolysate and extracts (Fig. 5 and see supplementary materials). In SWE I, the increased degree of substitution of AX as a function of time was marked by the enrichment of the C(O)-3 linked Xylp (3,4-Xylp), which is the most abundant motif found in wheat AX (Saulnier et al., 2007). As AX was enriched in E-I-30', the molar mass distribution also showed a more unimodal peak at around 10^4 Da (Fig. 5b). The removal of small (10^3 Da) and large (10^5 – 10^6 Da) populations in E-I-5' further implied that sequential extraction in SWE I could remove small molecular compounds and starch, respectively.

After enzymatic treatment, a substantial increase of terminal Xylp (*t*-Xylp) was observed in the hydrolysates, which resulted from cleavage of

the xylan backbone (Fig. 5a). In ET-X10A-F, the amount of substituted Xylp was considerably less than of ET-X5_21-F, while the amount of *t*-Xylp was relatively higher. This corresponds well with the high abundance of X₂ in ET-X10A-F and the occurrence of longer and more substituted oligosaccharides in ET-X5_21-F (Fig. 4d). The high amount of *t*-Xylp was also reflected in the molar mass distribution of ET-X10A-F, as it exhibited a unimodal peak at 10^2 – 10^3 Da (Fig. 5c). For ET-X5_21-F, much larger populations were present (10^4 Da), inferring that the hydrolysate contained both longer oligosaccharides and polysaccharides.

Interestingly in SWE II after enzymatic treatment, E-II-X10A-F was much more substituted than ET-X5_21-F, having almost equal amounts of both single (3,4-Xylp and 2,4-Xylp) and double substitutions (2,3,4-Xylp) (Fig. 5a). The increase in substitution coincided with the increase of A/X ratio in Wb-R-10A-F after enzymatic treatment (Fig. 4f), where extracts exhibiting high substitution was somewhat expected. The E-II-X10A-F also resulted in a higher amount of *t*-Xylp than ET-X5_21-F, inferring that Wb-R-10A-F was cleaved at several points. SEC analysis confirmed that E-II-X10A-F displayed a unimodal peak at around 10^3 – 10^4 (Fig. 5d), suggesting that the extracted AXs were still in polymeric form. Meanwhile, the molar mass distribution was slightly lower for ET-X5_21-F than E-II-X10A-F, which was surprising since the former exhibited a lower amount of *t*-Xylp. This result suggested that the E-II-X10A-F, although cleaved at the backbone, could have still been cross-

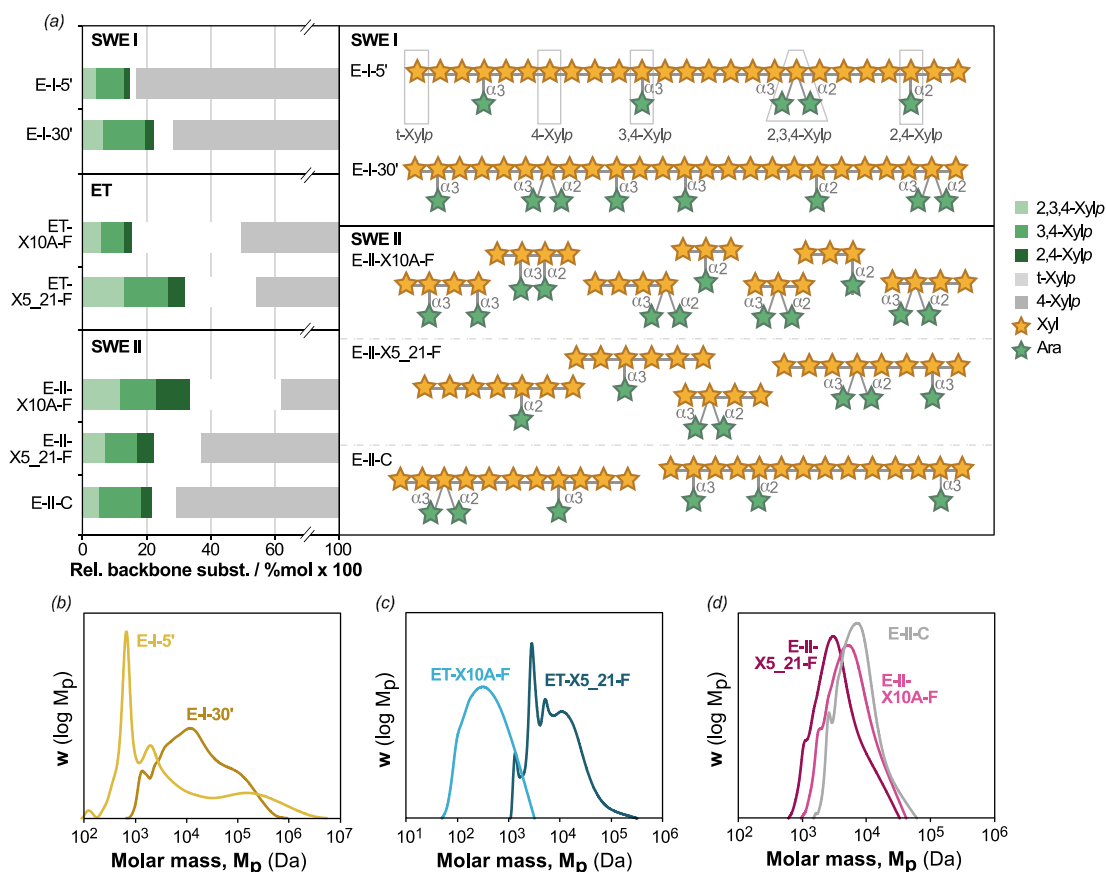


Fig. 5. Molecular characterisation of soluble fractions from the bioprocess. (a) Substitution pattern of xylan backbone from soluble fractions based on glycosidic linkage analysis. Here it was assumed that the majority of the substitution was accounted by Ara_f. Molar mass distribution of soluble fractions from (b) SWE I, (c) Enzymatic treatment (ET) and (d) SWE II.

linked by the diFAs, explaining the higher molar mass. Indeed, E-II-X10A-F contained higher amount of diFAs (5,5' and 8,8' diFA) at 1.5 mg/g compared to the ET-X5_21-F (Fig. 4i). It was likely that other forms of diFAs were present in the samples, thus further supporting the notion.

To confirm this, the released phenolic acids were analysed using LC-ESI-MS by selecting the 369 *m/z* ion that corresponded to the *m/z* of diFA with the loss of one water molecule. The ion extracted chromatograms (see [supplementary materials](#)) revealed that several different peaks were

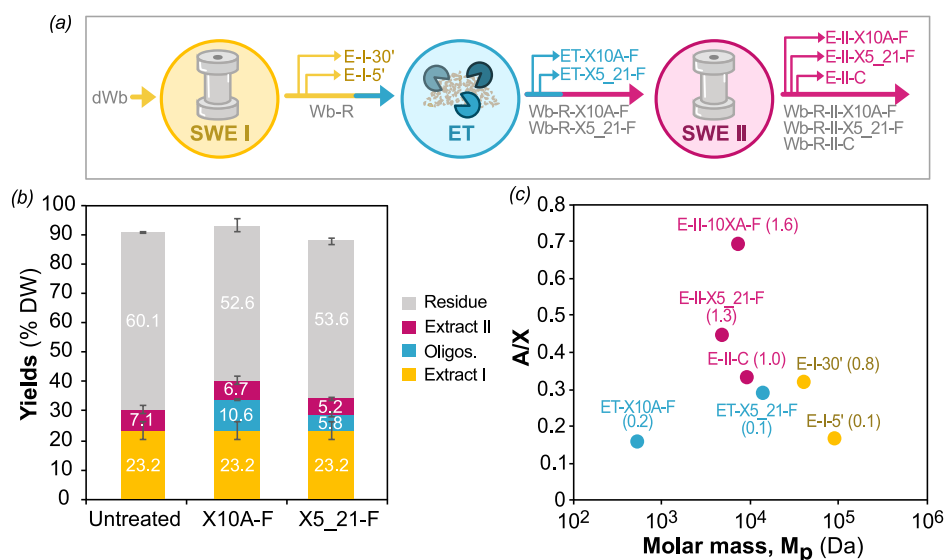


Fig. 6. Overview of integrated process in terms of yields and molecular structure. (a) Summary of fractions produced from the different steps of the bioprocess. (b) Total yields of extracts and residue of the whole integrated bioprocess in terms of starting wheat bran. (c) Plot depicting the molecular structure of soluble fractions from SWE I (yellow), enzymatic treatment (blue) and SWE II (pink) as a function of molar mass vs arabinose to xylose ratio. The values in brackets represents measured diFAs in mg/g. (For interpretation of the references to colour in this figure legend, the reader is referred to the web version of this article.)

present, which confirmed that were indeed more than two types of diFAs in the extracts. By referring to previous fragmentation spectra (Vismeh et al., 2013) in LC-ESI-MSⁿ, the presence of 8-O-4' diFA and 8-5' diFA was confirmed.

As for the insoluble Wb fractions, changes in the substitution pattern of AX that remained in the Wb were more prominent for X10A-F compared to X5_21-F (see supplementary materials). For instance, after enzymatic treatment, the Wb-R-10A-F exhibited an increase in the A/X ratio, which was caused by a large increase in the double substitution (2,3,4-Xylp). After SWE II, the overall A/X decreased in Wb-R-II-X10A-F (in agreement with the release of highly substituted AX in E-II-X10A-F) and this was mainly caused by a reduction of the double substitution. A majority portion of the double substitution may have been removed during SWE II; however, this motif was still the most prominent in the final residue of Wb-R-II-X10A-F, implying that it may play a fundamental role in the recalcitrance of Wb-R. As expected, the residues of Wb were also gradually enriched with cellulose, along with decreasing content of AX, as the bioprocess progressed.

The combination of SWE and enzymatic treatment improved the yields of AX extraction and provided different AX fractions with specific molecular structures of interest (Fig. 6). In terms of combined yields (Fig. 6b), SWE I yielded the highest value (23 %, in respect to the whole process) as the majority of accessible components (starch, mixed linked β -glucans and AX) were obtained in this step. Subsequently, enzymatic treatment on Wb-R from SWE I resulted in a higher hydrolysate yield by X10A-F (11 %) compared to X5_21-F (6 %). The highly active and broad specificity of AcXyn10A CBM1 enhanced oligosaccharide release, while the lower yield by CXyn5_21 was likely due to its limited specificity. The Wb-R treated with X10A-F released more extract (7 %) than the X5_21-F (5 %) in SWE II, implying that in terms of yields, the GH10 outperformed the GH5 xylanase.

As a by-product of the process, unextractable residues were co-produced at the end of SWE II (Fig. 6a). These residues were composed of 226–260 mg/g AX, 211–284 mg/g glucose (mostly cellulose as confirmed by linkage analysis), and plausibly lignin, protein and ash (Apprich et al., 2014; Stevenson et al., 2012). Based on the composition of the residue after the integrated bioprocess, it could be further utilised as a filler in material applications, as a feed substrate, or for bioenergy applications (either through bioethanol production through saccharification or biogas production). Indeed, subcritical water processing has been shown to increase the saccharification rates from lignocellulosic biomass as an alternative to conventional acid pretreatment (Sivan et al., 2023).

By calculating the amount of AX that remained in the final residues in respect to the initial dWb, the Wb-R-II-10A-F, Wb-R-II-5_21-F and Wb-R-II-C were left with 26, 30 and 33 % of AX, respectively. This indicated that the integrated bioprocess could extract the majority of AX present in dWb (i.e. up to 74 % for X10A-F), and the addition of enzymes greatly improved the AX yield, especially when X10A-F was used in the process. The total yields by the integrated bioprocess were significantly higher than those obtained by other studies using only enzymatic treatments, which were in the order of 5–10 % of the total AX present in destarched wheat bran (Aguedo et al., 2014; Santala et al., 2011) or by only using hydrothermal processing, in the range of 20–25 % of the total AX content (Aguedo et al., 2014; Li et al., 2020). The obtained AX yields are also slightly lower to those obtained through conventional alkaline extraction using NaOH or Ba(OH)₂, in the range of 45–70 % (Li et al., 2020; Ruthes et al., 2017), with the disadvantage that the alkaline treatment cleaves the ferulic acid moieties from the polysaccharide core.

Another added value from the different steps of the process is that each step resulted in an AX population with distinct molecular structures in terms of substitution pattern (A/X ratio), molar mass and ferulic acid content (Fig. 6c), which could in turn be developed into different applications. The fractions derived from the enzymatic treatments (ET) exhibited low molar mass and low A/X ratios, as shown in blue. On the other hand, the initial extracts after SWE I (yellow) exhibited the highest

molar mass distributions at around 10⁵ Da with low A/X ratio, between 0.2 and 0.3 depending on the extraction time. Finally, the SWE II extracts (in pink), exhibited moderate molar mass distributions at around 10⁴ Da, with higher A/X ratios (between 0.4 and 0.7) and a marked enrichment of diFAs. Here, we propose that the diFAs may play a role in holding the cleaved AX chains together, explaining the slightly relatively high molar mass of E-II-10A-F. The differences in length and degree of substitution are important for subsequent applications. The soluble and linear xylooligosaccharide fractions from ET could have potential use as prebiotic components in nutraceutical formulations, targeting the growth of beneficial gut bacteria and the production of derived metabolites such as short-chain fatty acids, as shown in recent reviews (Pang et al., 2023; Zannini et al., 2022). On the other hand, the longer AXs from SWE I and II are more suitable for structural food and material applications where both functional properties (as viscosity, gelling or film forming properties) and bioactivity are desired. The degree of substitution, which differs greatly among the steps, also impact digestibility by gut microbes (Broekaert et al., 2011), as well as solubility and oxygen permeability in materials (Höjje et al., 2008; Yilmaz-Turan et al., 2020). Moreover, the presence of phenolic acids both in bound and free form can contribute to additional antioxidant activity (Kikuzaki et al., 2002), with important nutritional and biomedical potential applications (Yilmaz-Turan et al., 2022).

The economic feasibility of the integrated bioprocess seems demonstrated based on the high yields of the process (345 g AX per kg of initial wheat bran) and the potential price of the purified AX and oligosaccharides. A previous study on the techno-economic feasibility of producing sugars from brewer spent grain using subcritical water reported costs of manufacturing between 2 and 10 USD kg⁻¹ for the most abundant sugars present in BSG (Sganzerla et al., 2021). However, a full techno-economic feasibility study should be performed, taking into account the process scale conditions and the potential business models for the targeted applications.

4. Conclusions

This study provides molecular insights into the use of xylanolytic enzymes and subcritical water extraction (SWE) for the maximised recovery of arabinoxylan (AX) polymers and oligosaccharides from wheat bran. Total AX yields of 74 % can be extracted by the integrated bioprocess, resulting in unique AX fractions with specific molecular structures in terms of degree of substitution (A/X ratios between 0.2 and 0.7), molecular weight (between 1 and 100 kDa) and ferulic acid content (between 1 and 12 mg/g). The xylooligosaccharides could be used in nutraceutical and prebiotic applications, whereas the polymeric AX could be used as matrices for biomaterials and functional food and cosmetic ingredients. This study contributes to the circularity of the food system through upcycling of underutilised agricultural side streams into valuable bioproducts.

CRedit authorship contribution statement

Reskandi C. Rudjito: Writing – original draft, Methodology, Investigation, Formal analysis, Data curation. **Alvaro C. Matute:** Writing – review & editing, Investigation. **Amparo Jiménez-Quero:** Writing – review & editing, Supervision, Methodology, Investigation. **Lisbeth Olsson:** Writing – review & editing, Conceptualization. **Mary Ann Stringer:** Investigation, Resources, Writing – review & editing. **Kristian Bertel Rømer Mørkeberg Krogh:** Conceptualization, Resources, Writing – review & editing. **Jens Eklöf:** Writing – review & editing, Resources, Conceptualization. **Francisco Vilaplana:** Writing – review & editing, Supervision, Resources, Project administration, Methodology, Funding acquisition, Formal analysis, Conceptualization.

Declaration of competing interest

The authors declare the following financial interests/personal relationships which may be considered as potential competing interests: Francisco Vilaplana reports financial support was provided by Swedish Research Council Formas. Francisco Vilaplana reports financial support was provided by Lantmännen Research Foundation. Francisco Vilaplana reports a relationship with Oatly AB that includes: employment. Mary Ann STRINGER reports a relationship with Novozymes that includes: employment. Kristian Bertel Romer Morkeberg Krogh reports a relationship with Novozymes that includes: employment. Jens Eklof reports a relationship with Novozymes that includes: employment. Francisco Vilaplana has patent #WO2016198651A3 issued to Lantmännen. If there are other authors, they declare that they have no known competing financial interests or personal relationships that could have appeared to influence the work reported in this paper.

Data availability

Data will be made available on request.

Acknowledgements

This work was funded by the Swedish Research Council Formas (Project 942-2016-119) and the Lantmännen Research Foundation (Project 2016F008). We would also like to acknowledge Dr. Annelie Moldin (Lantmännen) for providing us the wheat bran and for her valuable insight into the study.

Appendix A. Supplementary data

Supplementary data to this article can be found online at <https://doi.org/10.1016/j.biortech.2024.130387>.

References

- Aguedo, M., Fougny, C., Dermience, M., Richel, A., 2014. Extraction by three processes of arabinoxylans from wheat bran and characterization of the fractions obtained. *Carbohydr. Polym.* 105, 317–324.
- Alokika, Singh, B., 2019. Production, characteristics, and biotechnological applications of microbial xylanases. *Appl. Microbiol. Biotechnol.* 103 (21), 8763–8784.
- Antoine, C., Peyron, S., Mabilbe, F., Lapiere, C., Bouchet, B., Abecassis, J., Rouau, X., 2003. Individual contribution of grain outer layers and their cell wall structure to the mechanical properties of wheat bran. *J. Agric. Food Chem.* 51 (7), 2026–2033.
- Apprich, S., Tirpanalan, Ö., Hell, J., Reisinger, M., Böhmendorfer, S., Siebenhandl-Ehn, S., Novalin, S., Kneifel, W., 2014. Wheat bran-based biorefinery 2: Valorization of products. *LWT Food Sci. Technol.* 56 (2), 222–231.
- Broekaert, W., Courtin, C., Verbeke, K., Van De Wiele, T., Verstraete, W., Delcour, J., 2011. Prebiotic and Other Health-Related Effects of Cereal-Derived Arabinoxylans, Arabinoxylan-Oligosaccharides, and Xylooligosaccharides. *Crit. Rev. Food Sci. Nutr.* 51 (2), 178–194.
- Comino, P., Collins, H., Lahnstein, J., Beahan, C., Gidley, M.J., 2014. Characterisation of soluble and insoluble cell wall fractions from rye, wheat and hull-less barley endosperm flours. *Food Hydrocoll.* 41, 219–226.
- Correia, M.A.S., Mazumder, K., Brás, J.L.A., Firbank, S.J., Zhu, Y., Lewis, R.J., York, W. S., Fontes, C.M.G.A., Gilbert, H.J., 2011. Structure and function of an arabinoxylan-specific xylanase. *J. Biol. Chem.* 286 (25), 22510–22520.
- Crepin, V.F., Faulds, C.B., Connerton, I.F., 2004. Functional classification of the microbial feruloyl esterases. *Appl. Microbiol. Biotechnol.* 63 (6), 647–652.
- Falck, P., Aronsson, A., Grey, C., Ståhlbrand, H., Nordberg Karlsson, E., Adlercreutz, P., 2014. Production of arabinoxylan-oligosaccharide mixtures of varying composition from rye bran by a combination of process conditions and type of xylanase. *Bioresour. Technol.* 174, 118–125.
- FAO, 2021. *FAO Cereal Supply and Demand Brief*, Vol. 2021, FAO.
- Faulds, C.B., Zanichelli, D., Crepin, V.F., Connerton, I.F., Juge, N., Bhat, M.K., Waldron, K.W., 2003. Specificity of feruloyl esterases for water-extractable and water-unextractable feruloylated polysaccharides: influence of xylanase. *J. Cereal Sci.* 38 (3), 281–288.
- Faulds, C.B., Mandalari, G., LoCurto, R., Bisignano, G., Waldron, K.W., 2004. Arabinoxylan and mono- and dimeric ferulic acid release from brewer's grain and wheat bran by feruloyl esterases and glycosyl hydrolases from *Humicola insolens*. *Appl. Microbiol. Biotechnol.* 64 (5), 644–650.
- Faulds, C.B., Mandalari, G., Lo Curto, R.B., Bisignano, G., Christakopoulos, P., Waldron, K.W., 2006. Synergy between xylanases from glycoside hydrolase family 10 and family 11 and a feruloyl esterase in the release of phenolic acids from cereal arabinoxylan. *Appl. Microbiol. Biotechnol.* 71 (5), 622–629.
- Gallardo, C., Jiménez, L., García-Conesa, M.T., 2006. Hydroxycinnamic acid composition and in vitro antioxidant activity of selected grain fractions. *Food Chem.* 99 (3), 455–463.
- Grabber, J.H., Hatfield, R.D., Ralph, J., 1998. Diferulate cross-links impede the enzymatic degradation of non-lignified maize walls. *J. Sci. Food Agric.* 77 (2), 193–200.
- Grootaert, C., Delcour, J.A., Courtin, C.M., Broekaert, W.F., Verstraete, W., Van de Wiele, T., 2007. Microbial metabolism and prebiotic potency of arabinoxylan oligosaccharides in the human intestine. *Trends Food Sci. Technol.* 18 (2), 64–71.
- Höije, A., Sternemalm, E., Heikkinen, S., Tenkanen, M., Gatenholm, P., 2008. Material properties of films from enzymatically tailored arabinoxylans. *Biomacromolecules* 9 (7), 2042.
- Iiyama, K., Lam, T.B.T., Stone, B.A., 1994. Covalent cross-links in the cell wall. *Plant Physiol.* 104, 314–320.
- Izidorczyk, M.S., Biliaderis, C.G., 2000. Structural and functional aspects of cereal arabinoxylans and β -glucans. *Dev. Food Sci.* 41 (C), 361–384.
- Kikuzaki, H., Hisamoto, M., Hirose, K., Akiyama, K., Taniguchi, H., 2002. Antioxidant properties of ferulic acid and its related compounds. *J. Agric. Food Chem.* 50 (7), 2161–2168.
- Lehtio, J., Sugiyama, J., Gustavsson, M., Fransson, L., Linder, M., Teeri, T.T., 2003. The Binding Specificity and Affinity Determinants of Family 1 and Family 3 Cellulose Binding Modules. *PNAS* 100 (2), 484–489.
- Li, C., Wang, L., Chen, Z., Li, Y., Li, J., 2020. Facile and green preparation of diverse arabinoxylan hydrogels from wheat bran by combining subcritical water and enzymatic crosslinking. *Carbohydr. Polym.* 241, 116317.
- McKee, L.S., Sunner, H., Anasontzis, G.E., Toriz, G., Gatenholm, P., Bulone, V., Vilaplana, F., Olsson, L., 2016. A GH115 alpha-glucuronidase from *Schizophyllum commune* contributes to the synergistic enzymatic deconstruction of softwood glucuronoarabinoxylan. *Biotechnol. Biofuels* 9 (2), 1–13.
- McKee, L.S., 2017. *Measuring Enzyme Kinetics of Glycoside Hydrolases Using the 3,5-Dinitrosalicylic Acid Assay*. 1 ed. in: *Protein-Carbohydrate Interactions*, (Eds.) D.W. Abbott, A. Lammerts van Bueren, Humana Press, pp. XIII, 311.
- Mendez-Encinas, M.A., Carvajal-Millán, E., Rascon-Chu, A., Astiazaran-Garcia, H.F., Valencia-Rivera, D.E., 2018. Ferulated Arabinoxylans and Their Gels: Functional Properties and Potential Application as Antioxidant and Anticancer Agent. *Oxid. Med. Cell. Longev.* 2018, 1–23.
- Menzel, C., González-Martínez, C., Chiralt, A., Vilaplana, F., 2019. Antioxidant starch films containing sunflower hull extracts. *Carbohydr. Polym.* 214, 142–151.
- Miller, G.L., 1959. Use of dinitrosalicylic acid reagent for determination of reducing sugar. *Anal. Chem.* 31 (3), 426–428.
- Niño-Medina, G., Carvajal-Millán, E., Lizardi, J., Rascon-Chu, A., Marquez-Escalante, J. A., Gardea, A., Martínez-López, A.L., Guerrero, V., 2009. Maize processing waste water arabinoxylans: Gelling capability and cross-linking content. *Food Chem.* 115 (4), 1286–1290.
- Notenboom, V., Boraston, A.B., Williams, S.J., Kilburn, D.G., Rose, D.R., 2002. High-Resolution Crystal Structures of the Lectin-like Xylan Binding Domain from *Streptomyces lividans* Xylanase 10A with Bound Substrates Reveal a Novel Mode of Xylan Binding. *Biochemistry* 41 (13), 4246–4254.
- Paës, G., Berrin, J.-G., Beaugrand, J., 2012. GH11 xylanases: Structure/function/properties relationships and applications. *Biotechnol. Adv.* 30 (3), 564–592.
- Pang, J., Zhang, Y., Tong, X., Zhong, Y., Kong, F., Li, D., Liu, X., Qiao, Y., 2023. Recent Developments in Molecular Characterization, Bioactivity, and Application of Arabinoxylans from Different Sources. *Polymers* 15.
- Peterson, A.A., Vogel, F., Lachance, R.P., Fröling, M., Antal, J.M.J., Tester, J.W., 2008. Thermochemical biofuel production in hydrothermal media: A review of sub- and supercritical water technologies. *Energ. Environ. Sci.* 1 (1), 32–65.
- Petolino, F.A., Walsh, C., Fincher, G.B., Bacic, A., 2012. Determining the polysaccharide composition of plant cell walls. *Nat. Protoc.* 7 (9), 1590.
- Pollet, A., Delcour, J.A., Courtin, C.M., 2010. Structural determinants of the substrate specificities of xylanases from different glycoside hydrolase families. *Crit. Rev. Biotechnol.* 30 (3), 176–191.
- Pomeranz, Y., 1988. *Chemical composition of kernel structures*. in: *Wheat: chemistry and technology*, (Ed.) Y. Pomeranz, Springer, Berlin, pp. 99.
- Prückler, M., Siebenhandl-Ehn, S., Apprich, S., Höltinger, S., Haas, C., Schmid, E., Kneifel, W., 2014. Wheat bran-based biorefinery 1: Composition of wheat bran and strategies of functionalization. *LWT Food Sci. Technol.* 56 (2), 211–221.
- Reisinger, M., Tirpanalan, Ö., Prückler, M., Huber, F., Kneifel, W., Novalin, S., 2013. Wheat bran biorefinery – A detailed investigation on hydrothermal and enzymatic treatment. *Bioresour. Technol.* 144, 179–185.
- Rudjito, R.C., Ruthes, A.C., Jimenez-Quero, A., Vilaplana, F., 2019. Feruloylated Arabinoxylans from Wheat Bran: Optimization of Extraction Process and Validation at Pilot Scale. *ACS Sustain. Chem. Eng.* 7, 13167–13177.
- Rudjito, R.C., Jimenez-Quero, A., Hamzaoui, M., Kohnen, S., Vilaplana, F., 2020. Tuning the molar mass and substitution pattern of complex xylans from corn fibre using subcritical water extraction. *Green Chem.* 22 (23), 8337.
- Rudjito, R.C., Jiménez-Quero, A., Muñoz, M.D.C.C., Kull, T., Olsson, L., Stringer, M.A., Krogh, K.B.R.M., Eklöf, J., Vilaplana, F., 2023. Arabinoxylan source and xylanase specificity influence the production of oligosaccharides with prebiotic potential. *Carbohydr. Polym.* 320, 121233.
- Ruthes, A.C., Martínez-Abad, A., Tan, H.-T., Bulone, V., Vilaplana, F., 2017. Sequential fractionation of feruloylated hemicelluloses and oligosaccharides from wheat bran using subcritical water and xylanolytic enzymes. *Green Chem.* 19 (8), 1919–1931.

- Saeman, J.F.M., Wayne, E., Mitchell, R.L., Millett, M.A., 1954. Techniques for the determination of pulp constituents by quantitative paper chromatography. *Tappi J.* 37 (8), 336–343.
- Santala, O., Lehtinen, P., Nordlund, E., Suortti, T., Poutanen, K., 2011. Impact of water content on the solubilisation of arabinoxylan during xylanase treatment of wheat bran. *J. Cereal Sci.* 54 (2), 187–194.
- Saulnier, L., Sado, P.-E., Branlard, G., Charmet, G., Guillon, F., 2007. Wheat arabinoxylans: Exploiting variation in amount and composition to develop enhanced varieties. *J. Cereal Sci.* 46 (3), 261–281.
- Schooneveld-Bergmans, M.E.F., Beldman, G., Voragen, A.G.J., 1999. Structural Features of (Glucurono)Arabinoxylans Extracted from Wheat Bran by Barium Hydroxide. *J. Cereal Sci.* 29 (1), 63–75.
- Sganzerla, W.G., Zobot, G.L., Torres-Mayanga, P.C., Buller, L.S., Mussatto, S.I., Forster-Carneiro, T., 2021. Techno-economic assessment of subcritical water hydrolysis process for sugars production from brewer's spent grains. *Ind. Crop Prod.* 171, 113836.
- Sivan, P., Heinonen, E., Latha Gandla, M., Jiménez-Quero, A., Özeren, H.D., Jönsson, L. J., Mellerowicz, E.J., Vilaplana, F., 2023. Sequential extraction of hemicelluloses by subcritical water improves saccharification of hybrid aspen wood grown in greenhouse and field conditions. *Green Chem.*
- Stevenson, L., Phillips, F., Sullivan, K., Walton, J., 2012. Wheat bran: its composition and benefits to health, a European perspective. *International Journal of Food Sciences and Nutrition*, 2012, 63(8), p.1001-1013, 63(8), 1001-1013.
- Vismeh, R., Lu, F., Chundawat, S.P.S., Humpala, J.F., Azarpira, A., Balan, V., Dale, B.E., Ralph, J., Jones, A.D., 2013. Profiling of diferulates (plant cell wall cross-linkers) using ultrahigh-performance liquid chromatography-tandem mass spectrometry. *Analyst* 138 (21), 6683–6692.
- Yilmaz-Turan, S., Jiménez-Quero, A., Menzel, C., de Carvalho, D.M., Lindström, M.E., Sevastyanova, O., Moriana, R., Vilaplana, F., 2020. Bio-based films from wheat bran feruloylated arabinoxylan: Effect of extraction technique, acetylation and feruloylation. *Carbohydr. Polym.* 250, 116916.
- Yilmaz-Turan, S., Jiang, K., Lopez-Sanchez, P., Jiménez-Quero, A., Crouzier, T., Plivelic, T.S., Vilaplana, F., 2022. Hydrogels with protective effects against cellular oxidative stress via enzymatic crosslinking of feruloylated arabinoxylan from corn fibre. *Green Chem.* 24 (23), 9114–9127.
- Zannini, E., Bravo Núñez, Á., Sahin, A.W., Arendt, E.K., 2022. Arabinoxylans as Functional Food Ingredients: A Review. *Foods* 11 (7), 1026.